# Derivation and characteristics analysis of an acoustics–convection upstream resolution algorithm for the two-dimensional Euler and Navier–Stokes equations

## Joe Iannelli[*,†,‡]

*Centre for Aeronautics, School of Engineering and Mathematical Sciences, City University, Northampton Square, London EC1V 0HB, U.K.*

### SUMMARY

The first of a two-paper series, this paper introduces a new decomposition not of the hyperbolic flux vector but of the flux vector Jacobian. The paper then details for the Euler and Navier–Stokes equations an intrinsically infinite directional upstream-bias formulation that rests on the mathematics and physics of multi-dimensional acoustics and convection. Based upon characteristic velocities, this formulation introduces the upstream bias directly at the differential equation level, before the spatial discretization, within a characteristics-bias governing system. Through a decomposition of the Euler flux divergence into multi-dimensional acoustics and convection–acoustics components, this characteristics-bias system induces consistent upstream bias along all directions of spatial wave propagation, with anisotropic variable-strength upstreaming that correlates with the spatial distribution of characteristic velocities. Copyright © 2005 John Wiley & Sons, Ltd.

KEY WORDS: Euler and Navier–Stokes equations; CFD; characteristics; multi-dimensional upwind

## 1. INTRODUCTION

This paper provides the first part of a two-part investigation into the development of continuum, i.e. non-discrete, multi-dimensional and infinite-directional characteristics-bias approximations of the Euler and Navier–Stokes equations and subsequent computational implementation. The second part [1], also featured in this Journal, presents a finite element and implicit Runge–Kutta implementation and applications to smooth and shocked aerodynamic and gas dynamic transonic and supersonic flows. This paper details the development and characteristics analysis of the Acoustic–Convection Upstream Resolution algorithm.

---

[*]Correspondence to: Joe Iannelli, Centre for Aeronautics, School of Engineering and Mathematical Sciences, City University, Northampton Square, London EC1V 0HB, U.K.
[†]E-mail: g.iannelli@city.ac.uk
[‡]Director.

Multi-dimensional upwind Euler and Navier–Stokes solvers remain of considerable interest computationally to investigate realistic flows on arbitrary grids. Numerous finite element, difference and volume algorithms have progressed somewhat independently from the physics of acoustics and convection, the wave propagation mechanisms within gas dynamic flows. The dissipation mechanisms, or upwind schemes, within these algorithms have been developed at the discrete level, in connection with a specific grid or pattern of computational cells.

Several finite element solvers have either utilized modifications of the test space or introduced Taylor's series-based dissipation terms [2] to generate stable algorithms. The mathematical developments in these fundamental contributions have remained independent of characteristics theory. Upwind finite element methods for scalar equations have also been developed [3] including the Streamline Upwind Petrov–Galerkin (SUPG) formulation [4–8], also known as the streamline diffusion (SD) method [5]. Extensions to systems are recognized to remain heuristic, the induced upwinding is not necessarily in the streamline direction, and additional 'shock capturing' terms are needed for computing essentially non-oscillatory shocked flows [9].

Intense research is also focused on multi-dimensional finite-volume upwind schemes that induce upwinding along a few significant directions. An early effort [10] generated a grid-independent upwind scheme based on directional upwinding along possible shock wave directions. This approach later enjoyed addition of local Riemann solutions [11] along several upwind directions including the flow-velocity, speed-gradient and pressure-gradient directions. An alternative second-order rotated upwind scheme [12] used flux-difference splitting (FDS) along two orthogonal directions determined on the basis of the local pressure gradient. Other approaches involved approximate multi-dimensional Riemann solvers and local wave decompositions, with wave modelling [13–16]. In these formulations, some wave directions and strengths are fixed *a priori* to generate a viable CFD algorithm.

Difficulties remain in these methods both in assessing the magnitude of the induced multi-dimensional upwind diffusion and determining whether consistent upwinding exists not only over the selected directions, but along all flow-field wave-propagation directions. Additional data filtering or upwind-direction freezing may also be required for convergence and essential monotonicity. More fundamentally, current multi-dimensional upwind schemes are recognized to rest upon much less theoretical support than their one-dimensional counterparts [17].

This two-part presentation expounds the multi-dimensional formulation of the acoustics–convection upstream resolution Euler solver introduced in Reference [18]. That reference article documented the algorithm for the quasi-one-dimensional Euler equations. The organization of that article is followed in this paper, which begins by describing an alternative multi-dimensional upstream-bias formulation that encompasses and generalizes both flux-vector and FDS schemes. Named flux Jacobian decomposition (FJD) and developed for multi-dimensional hyperbolic and parabolic systems, this decomposition splits not the flux vector, but rather the flux Jacobian. An upstream-bias integral average of the FJD along principal wave-propagation directions then directly yields not only an intrinsically multi-dimensional upstream-bias formulation, but also an associated necessary stability condition. Applied to a general multidimensional hyperbolic or parabolic system, the combination of FJD and upstream-bias integral averaging generates the upstream-bias approximation directly at the differential equation level, before any discretization, within a 'companion' characteristics-bias system associated with the governing system. A conventional centred or finite element Galerkin spatial

*Int. J. Numer. Meth. Fluids* 2005; **49**:1233–1260

approximation of this companion system then automatically and directly generates a genuinely multi-dimensional upstream-bias discrete analogue of the given system [1].

Developed for the multi-dimensional Euler and Navier–Stokes equations with general equilibrium equations of state, the acoustics–convection upstream resolution algorithm consists of a specific instance of FJD and integral averaging, an instance that rests on a decomposition of the multi-dimensional Euler Jacobian into matrix components that physically represent multi-dimensional acoustics and convection, the wave propagation mechanisms within gas dynamic flows. In particular, this development reveals that no single decomposition of the Euler flux components themselves can contain separate terms that reflect multi-dimensional acoustics. This formulation induces the upstream bias along all flow-field directions of wave propagation and enjoys a consistent theoretical support that rests upon the mathematics and physics of multi-dimensional acoustic and convection characteristic wave propagation.

This paper is organized in seven sections. After the introductory considerations in Section 1, Sections 2 and 3 delineate both the Euler as well as Navier–Stokes equations and a reference polar characteristics analysis. This analysis provides the necessary background for the multi-dimensional non-discrete upstream-bias formulation, in Section 4, and acoustics–convection decomposition of the Euler flux divergence, in Section 5. Section 6 then details the multi-dimensionality and infinite directionality of the formulation, with Section 7 summarizing concluding remarks.

## 2. NAVIER–STOKES AND EULER EQUATIONS

With respect to an inertial Cartesian reference frame, with implied summation on repeated indices, the classical Navier–Stokes and Euler conservation law system [19, 20] is

$$\frac{\partial q}{\partial t} + \frac{\partial f_j(q)}{\partial x_j} - \frac{\partial f_j^v}{\partial x_j} = 0 \tag{1}$$

which consists of the continuity, linear-momentum and total-energy equations. For three-dimensional formulations, $1 \leqslant j \leqslant 3$, and with $\mathscr{R}$ denoting the real-number field, the independent variable $(\mathbf{x}, t)$, $\mathbf{x} \equiv (x_1, x_2, x_3)$, in (1) varies in the domain $D \equiv \Omega \times [t_o, t_f]$, $[t_o, t_f] \subset \mathscr{R}^+$, $\Omega \subset \mathscr{R}^3$. When the 'viscosity' flux $f_j^v$, $1 \leqslant j \leqslant 3$, identically vanishes, this system is hyperbolic when the eigenvalues of the Jacobian matrix $(\partial f_j(q)/\partial q)n_j$ are all real for arbitrary unit vectors $\mathbf{n}$ with direction cosines $n_j$, the components of $\mathbf{n}$ along the coordinate axes. The system is also termed 'strongly' hyperbolic when this matrix possess a full set of eigenvectors [21, 22]. With reference to Figure 1, for a representative 2-D flow, the unit vector $\mathbf{n}$ indicates in the flow field the propagation direction of plane waves with speeds equal to the eigenvalues of $(\partial f_j(q)/\partial q)n_j$, as elaborated in Section 3.

The figure also displays the unit vectors $\mathbf{a}$ and $\mathbf{a}^N$, respectively, pointing in the streamline and crossflow directions, vectors that provide the two principal directions for the decomposition developed in Sections 3–6. The integral formulation for system (1), [23, 24], seeks a solution $q \in \mathscr{H}^1(\Omega)$, subject to prescribed boundary conditions on $\partial\Omega \equiv \bar{\Omega}\backslash\Omega$, such that for all test functions $\hat{w} \in \mathscr{H}^1(\Omega)$

$$\int_\Omega \left( \hat{w}\frac{\partial q}{\partial t} + \hat{w}\frac{\partial f_j}{\partial x_j} - \frac{\partial \hat{w}}{\partial x_j}f_j^v \right) \mathrm{d}\Omega + \oint_{\partial\Omega} \hat{w}f_j^v n_j\,\mathrm{d}(\partial\Omega) = 0 \tag{2}$$
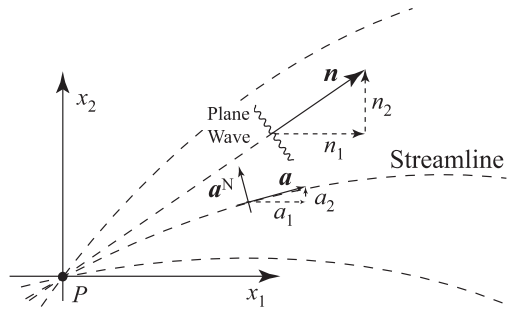
Figure 1. Reference unit vectors.

where $n_j$, $1 \leqslant j \leqslant 3$, denotes the $j$th component of the outward pointing unit vector perpendicular to $\partial\Omega$. For 2-D flows, $1 \leqslant j \leqslant 2$, the dependent-variable array $q = q(\mathbf{x}, t)$ as well as the inviscid and viscous flux 'vector' components $f_j$ and $f_j^v$ are then defined as

$$q \equiv \begin{Bmatrix} \rho \\ m_1 \\ m_2 \\ E \end{Bmatrix}, \quad f_1 \equiv \begin{Bmatrix} m_1 \\ \dfrac{m_1}{\rho} m_1 + p \\ \dfrac{m_1}{\rho} m_2 \\ \dfrac{m_1}{\rho}(E + p) \end{Bmatrix}, \quad f_2 \equiv \begin{Bmatrix} m_2 \\ \dfrac{m_2}{\rho} m_1 \\ \dfrac{m_2}{\rho} m_2 + p \\ \dfrac{m_2}{\rho}(E + p) \end{Bmatrix}, \quad f_j^v \equiv \begin{Bmatrix} 0 \\ \tau_{1j} \\ \tau_{2j} \\ \dfrac{m_i}{\rho} \tau_{ij} - q_j^{\mathscr{F}} \end{Bmatrix} \quad (3)$$

In the array $q$, the variables $\rho$, $m_1$, $m_2$, and $E$, respectively, denote static density and volume-specific linear momentum components and total energy. The Eulerian flow velocity $\mathbf{u}$, with Cartesian components $u_j$, $1 \leqslant j \leqslant 2$, is defined as $\mathbf{u} \equiv \mathbf{m}/\rho$. In the viscous flux $f_j^v$, the terms $\tau_{ij}$ and $q_j^{\mathscr{F}}$ [19], respectively, indicate the components of the deviatoric stress tensor and the component of the Fourier heat-conduction flux as

$$\tau_{ij} = \mu \left( \frac{\partial u_i}{\partial x_j} + \frac{\partial u_j}{\partial x_i} \right) + \bar{\lambda} \frac{\partial u_k}{\partial x_k} \delta_i^j, \quad q_j^{\mathscr{F}} = -k \frac{\partial T}{\partial x_j} \quad (4)$$

where $\mu$, $\bar{\lambda}$, $k$, and $T$, respectively, denote the first and second coefficient of dynamic viscosity, coefficient of thermal conductivity and static temperature. With respect to the two coefficients of viscosity, they are classically related by specifying equality between mechanical and thermodynamic pressure, which leads to $\bar{\lambda} = -2\mu/3$, traditionally known as Stokes' hypothesis [19].

   For any homogeneous equilibrium gas, pressure $p$ can be expressed as a function of two other thermodynamic variables [25]. They are density $\rho$ and mass-specific internal energy $\varepsilon$, in this case, since they are readily available from the Euler and Navier–Stokes system (1). The expressions for $\varepsilon$ and the pressure equation of state become

$$\varepsilon \equiv \frac{E}{\rho} - \frac{1}{2\rho^2}(m_1^2 + m_2^2), \quad p = p(\rho, \varepsilon) = p\left( \rho, \frac{E}{\rho} - \frac{1}{2\rho^2}(m_1^2 + m_2^2) \right) \quad (5)$$

According to this expression, the Jacobian derivatives of $p$ with respect to $q$, for the Jacobian $\partial f_j/\partial q$ of $f_j(q)$, are not all independent of one another. The derivatives of (5) with respect to $m_1$, $m_2$ and $E$ in fact satisfy the constraints

$$\left.\frac{\partial p}{\partial m_1}\right|_{\rho,m_2,E} = -\frac{m_1}{\rho}\left.\frac{\partial p}{\partial E}\right|_{\rho,m_1,m_2}, \qquad \left.\frac{\partial p}{\partial m_2}\right|_{\rho,m_1,E} = -\frac{m_2}{\rho}\left.\frac{\partial p}{\partial E}\right|_{\rho,m_1,m_2} \tag{6}$$

as obtained by expressing the derivatives of $p$ with respect to $m_1$, $m_2$ and $E$ in terms of the thermodynamic derivative of $p$ with respect to $\varepsilon$, from the first expression in (5). In the following sections, for simplicity, the abridged notation

$$p_\rho \equiv \left.\frac{\partial p}{\partial \rho}\right|_{m_1,m_2,E}, \qquad p_{m_1} \equiv \left.\frac{\partial p}{\partial m_1}\right|_{\rho,m_2 E}, \qquad p_{m_2} \equiv \left.\frac{\partial p}{\partial m_2}\right|_{\rho,m_1 E}, \qquad p_E \equiv \left.\frac{\partial p}{\partial E}\right|_{\rho,m_1,m_2} \tag{7}$$

will denote the Jacobian derivatives of pressure. The specific perfect-gas expressions for (5) follow from the internal energy and pressure equation of state as

$$\varepsilon = c_v T = \frac{R}{\gamma - 1}T, \quad p = \rho RT \ \Rightarrow \ p = (\gamma - 1)\rho\varepsilon = (\gamma - 1)\left(E - \frac{1}{2\rho}(m_1^2 + m_2^2)\right) \tag{8}$$

where $c_v$, $R$ and $\gamma = c_p/c_v$, $c_p - c_v = R$, respectively, denote the constant-volume specific heat, gas constant and specific-heat ratio. In terms of the Jacobian partial derivatives of $p$ for general equations of state, the square of the speed of sound $c$ and the corresponding mass-specific total enthalpy $H$ can be expressed as

$$c^2 \equiv \left.\frac{\partial p}{\partial \rho}\right|_S = p_\rho + p_E\left(\frac{E + p}{\rho} - \frac{1}{\rho^2}(m_1^2 + m_2^2)\right), \quad H = \frac{E + p}{\rho} = \frac{c^2(1 + p_E M^2) - p_\rho}{p_E} \tag{9}$$

where $M \equiv \|\mathbf{u}\|/c$ denotes the Mach number.

## 3. CHARACTERISTICS ANALYSIS

Within a 2-D flow field, acoustic and convection waves propagate in infinitely many directions, on the flow plane; along each direction the associated propagation velocity also depends on the Mach number. As an essential prerequisite for the developments in Section 4, this section presents an intrinsically multi-dimensional characteristics analysis based on a non-linear wave-like form of the solution $q$. This analysis leads to the spatial distribution of multi-dimensional propagation velocities and shows that among all propagation directions the streamline and crossflow directions are principal propagation directions. This line of enquiry is highlighted because it yields specific conditions for a physically coherent upstream bias formulation that remains consistent with multi-dimensional acoustic and convection wave propagation.

### 3.1. Characteristic velocity components

The non-linear wave-like form of $q$ is expressed as

$$q = q(\eta_1), \quad \eta_1 = \mathbf{x} \cdot \mathbf{n} - \lambda(q)t = x_j n_j - \lambda(q)t \tag{10}$$

where $\mathbf{n}$ denotes a space-domain propagation-direction unit vector, independent of $(\mathbf{x}, t)$, and $\lambda = \lambda(q)$ indicates a wave-propagation velocity component along the $\mathbf{n}$ direction. This solution-dependent velocity component is determined by enforcing the condition that the non-linear wave-like solution (10) satisfies the Euler equations. For non-linear $\lambda = \lambda(q)$ too [21, 22], this condition yields the eigenvalue problem

$$\left( -\lambda(q)I + \frac{\partial f_j}{\partial q} n_j \right) \frac{\partial q}{\partial \eta_1} = 0 \tag{11}$$

For non-trivial solutions $\partial q/\partial \eta_1$, hence non-trivial $q = q(\eta_1)$, the characteristic velocity components $\lambda$ are thus the eigenvalues of the linear combination of flux vector Jacobians

$$\frac{\partial f_j(q)}{\partial q} n_j = \begin{pmatrix} 0 & n_1 & n_2 & 0 \\ -u_1 u_j n_j + p_\rho n_1 & u_1 n_1 + u_j n_j + p_{m_1} n_1 & u_1 n_2 + p_{m_2} n_1 & p_E n_1 \\ -u_2 u_j n_j + p_\rho n_2 & u_2 n_1 + p_{m_1} n_2 & u_2 n_2 + u_j n_j + p_{m_2} n_2 & p_E n_2 \\ u_j n_j(p_\rho - H) & H n_1 + u_j n_j p_{m_1} & H n_2 + u_j n_j p_{m_2} & u_j n_j(1 + p_E) \end{pmatrix} \tag{12}$$

For general equations of state, these eigenvalues have been exactly determined in closed form as

$$\lambda_{1,2}^{d_E} = u_j n_j, \quad \lambda_{3,4}^{d_E} = u_j n_j \pm (p_\rho + p_E(H - u_j u_j))^{1/2} \tag{13}$$

where superscript $d_E$ signifies dimensional Euler eigenvalues. Of interest, eigenvalues $\lambda_{3,4}^{d_E}$ directly incorporate a sound speed expression that coincides with the isentropic partial derivative of pressure (9). Through such an expression, these equilibrium-gas eigenvalues become the well-known expressions

$$\lambda_{1,2}^{d_E} = u_j n_j, \quad \lambda_{3,4}^{d_E} = u_j n_j \pm c \tag{14}$$

which have the same familiar form as the perfect-gas eigenvalues. The non-dimensional form of (14) follows from division by $c$, which supplies the Mach-number-dependent expressions

$$\lambda_{1,2}^E = v_j n_j M, \quad \lambda_{3,4}^E = v_j n_j M \pm 1 \tag{15}$$

where $v_1$ and $v_2$ denote the components of a unit vector $\mathbf{v}$ in the velocity $\mathbf{u}$ direction.

As an elaboration over these expressions, the contraction $v_j n_j$, i.e. the inner product of the two unit vectors $\mathbf{n}$ and $\mathbf{v}$, is further expressed in terms of the cosine of the angle $(\theta - \theta_\mathbf{v})$ between $\mathbf{n}$ and $\mathbf{v}$, where $\theta$ and $\theta_\mathbf{v}$, respectively, denote the angle between $\mathbf{n}$ and the $x_1$-axis and the angle between $\mathbf{v}$ and the $x_1$-axis. Eigenvalues (15) thus become

$$\lambda_{1,2}^E = \cos(\theta - \theta_\mathbf{v})M, \quad \lambda_{3,4}^E = \cos(\theta - \theta_\mathbf{v})M \pm 1 \tag{16}$$

These expressions, in particular, imply that the Euler eigenvalues achieve their extrema for $\theta = \theta_\mathbf{v}$, hence when $\mathbf{n}$ points in the streamline direction, whereas for $\mathbf{n}$ pointing in the crossflow direction, hence $\theta = 90° + \theta_\mathbf{v}$, these eigenvalues no longer depend upon $M$.

The convection eigenvalues $\lambda_{1,2}^E$ vanish when $\cos(\theta - \theta_{\mathbf{v}}) = 0$, hence for $\mathbf{n}$ perpendicular to the streamline direction, or, equivalently, pointing in the crossflow direction. Since $\| \cos(\theta - \theta_{\mathbf{v}}) \| \leqslant 1$, the acoustic–convection eigenvalues $\lambda_{3,4}^E$ can only vanish for $M \geqslant 1$, hence for supersonic flows. For these flows, $\lambda_{3,4}^E = 0$ when

$$\mp \cos(\theta - \theta_{\mathbf{v}}) = \pm \sin((\theta - 90°) - \theta_{\mathbf{v}}) = \frac{1}{M} \qquad (17)$$

hence for $\mathbf{n}$ perpendicular to the Mach lines, for $\pm((\theta - 90°) - \theta_{\mathbf{v}})$ corresponds to the angle between a Mach line and the streamline, from the well-known second expression in (17). The lines that are perpendicular to the Mach lines will be called 'conjugate' lines.

The lines that are perpendicular to $\mathbf{n}$ for vanishing eigenvalues $\lambda_{1,2}^E$ and $\lambda_{3,4}^E$ thus, respectively, become the streamline and Mach lines. This result is not coincidental, for vanishing eigenvalues $\lambda_{1,4}^E$ correspond to wave-like solutions of the steady Euler equations, for which the streamline and Mach lines are characteristic-wave propagation lines.

### 3.2. Polar variation of characteristic speeds

As a novel way of visualizing the Euler eigenvalues, Figures 2 and 3 present the polar variation of the absolute values of eigenvalues (15) for subsonic, sonic and supersonic Mach numbers, in a neighbourhood of a flow field point $P$ in the $(x_1, x_2)$ plane. These variations are obtained for a variable unit vector $\mathbf{n} \equiv (\cos\theta, \sin\theta)$ and fixed unit vector $\mathbf{v}$, in this representative case inclined by $+30°$ with respect to the $x_1$-axis. A collective inspection of all these diagrams reveals three shared features for all Mach numbers. The maximum characteristic speeds occur in the velocity direction, i.e. along a streamline, as noted before. Secondly, all
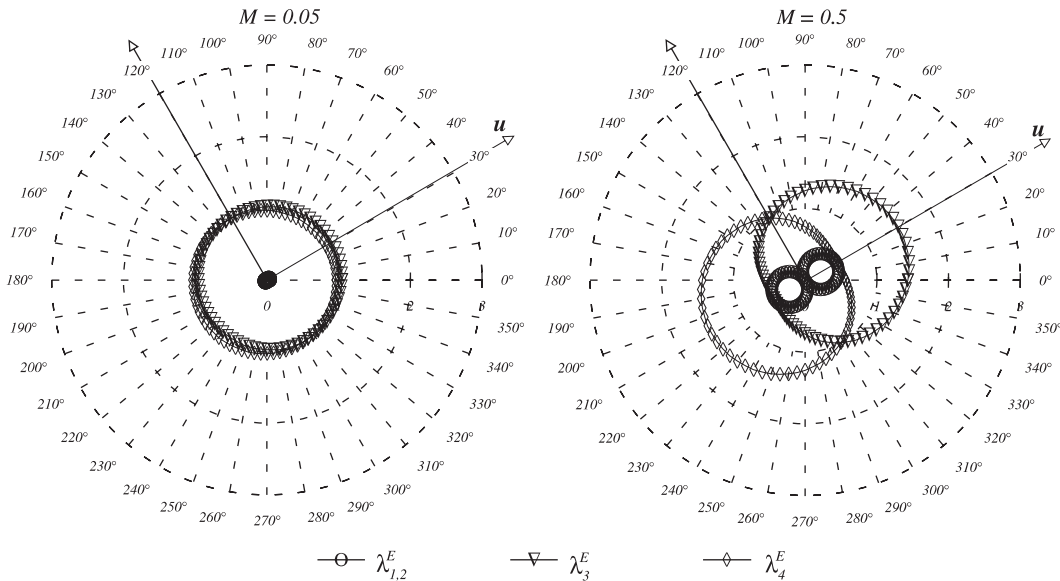


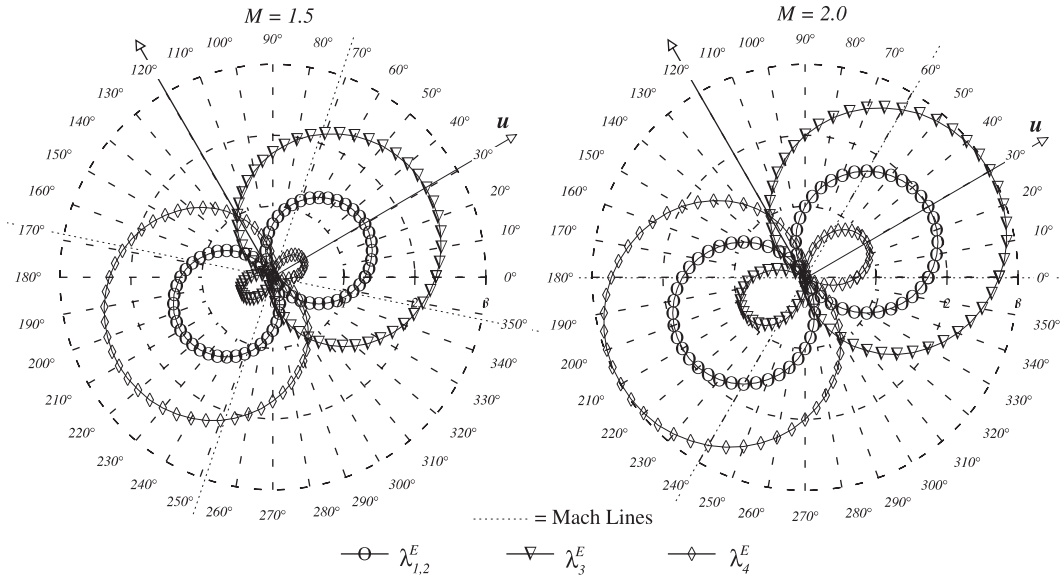Figure 2. Polar variation of subsonic wave speeds.

Figure 3. Polar variation of supersonic wave speeds.

the characteristic speeds are symmetrically distributed about the streamline direction. Thirdly, the eigenvalue pairs $(\|\lambda_1^E\|, \|\lambda_2^E\|)$ and $(\|\lambda_3^E\|, \|\lambda_4^E\|)$ remain mirror skew-symmetric with respect to the crossflow direction, in the sense that the curves representative of $\|\lambda_2^E\|$ and $\|\lambda_4^E\|$ become the respective mirror images of the variations of $\|\lambda_1^E\|$ and $\|\lambda_3^E\|$ with reference to this direction. The streamline and crossflow directions, therefore, become two fundamental wave-propagation axes.

For vanishing Mach numbers, the acoustic–convection propagation curves in the figure approach two circumferences. The distribution of propagation speeds in this case is therefore isotropic, which corresponds to the direction-invariant propagation of acoustic waves. As the Mach number increases from zero, the curves in the figure progressively become circular asymmetric, which corresponds to anisotropic wave propagation. For $M = 0.5$ this anisotropy is already evident and becomes more pronounced for higher Mach numbers. The non-dimensional characteristic speeds then approach 1 in the region about the crossflow direction, which corresponds to essentially acoustic propagation. For all Mach numbers, the convection eigenvalues $\lambda_{1,2}$ change sign when the **n** direction shifts from an upstream to a downstream axis with respect to **u**. For this reason, the associated curves cross the polar origin. Pure convective propagation, therefore, remains mono-axial, from upstream to downstream of $P$, and the axis of this type of wave propagation is the streamline.

For subsonic Mach numbers the acoustic–convection eigenvalues $\lambda_3^E$ and $\lambda_4^E$, respectively, remain positive and negative for all directions. For this reason the associated curves contain the polar origin. For subsonic flows, therefore, acoustic–convection waves propagate bi-modally, from both upstream and downstream toward and away from point $P$, along all directions radiating from $P$.

Beginning at the sonic state, this pattern drastically changes for supersonic Mach numbers, as illustrated in Figure 3. In this case both $\lambda_3^E$ and $\lambda_4^E$ change algebraic sign when the sense of $\mathbf{n}$ shifts from upstream to downstream of $P$ along a streamline. For this reason, the associated curves cross the polar origin. For supersonic flows, therefore, acoustic–convection wave propagation becomes mono-axial along a streamline, from upstream to downstream of $P$; nevertheless pure acoustic propagation remains bi-modal about the crossflow direction, for eigenvalues $\lambda_{3,4}^E$ remain of mixed algebraic sign outside the region that contains the streamline between the Mach lines. The following sections develop an upstream-bias formulation with magnitude of upstream bias that reflects this distribution of characteristic speeds about the streamline and crossflow directions.

## 4. NON-DISCRETE UPSTREAM-BIAS APPROXIMATION

The non-discrete upstream-bias approximation is developed for a non-linear hyperbolic or parabolic system

$$\frac{\partial q}{\partial t} + \frac{\partial f_j(q)}{\partial x_j} - \frac{\partial f_j^v}{\partial x_j} = 0 \qquad (18)$$

with implied summation on repeated subscript indices. When the 'viscosity' term $f_j^v$ identically vanishes, this system reduces to a first-order hyperbolic system. Equivalent to this governing system is the integral statement

$$\int_{\hat{\Omega}} \hat{w} \left( \frac{\partial q}{\partial t} + \frac{\partial f_j(q)}{\partial x_j} - \frac{\partial f_j^v}{\partial x_j} \right) d\Omega = 0 \qquad (19)$$

when it holds for arbitrary subdomains $\hat{\Omega} \subseteq \Omega$ and test functions $\hat{w} \in \mathscr{H}^1(\hat{\Omega}) \subseteq \mathscr{H}^1(\Omega)$ with compact support in $\hat{\Omega}$ [21, 22].

The non-discrete formulation induces a multi-dimensional upstream bias directly in the continuum, at the partial-differential equation level, before the eventual discretization on a prescribed grid. This continuum upstream-bias formulation derives from a characteristics-bias integral statement associated with (18). With reference to (19), the characteristic-bias integral is then defined as

$$\int_{\hat{\Omega}} \hat{w} \left( \frac{\partial q}{\partial t} + \frac{\partial f_j^C}{\partial x_j} - \frac{\partial f_j^v}{\partial x_j} \right) d\Omega = 0 \qquad (20)$$

where $f_j^C$ corresponds to a characteristics flux that automatically induces within (20) a multi-dimensional and infinite directional upstream-bias approximation for the hyperbolic flux divergence $\partial f_j / \partial x_j$. Most importantly, since the characteristics flux is developed independently and before any discretization, a genuinely multi-dimensional upstream-bias approximation for the governing equations (1), (18) on arbitrary grids directly results from a straightforward centred discretization of the characteristics flux on the given grid.

### 4.1. Characteristics-bias flux

To develop an intrinsically multi-dimensional and infinite-directional characteristics-bias flux $f_j^C$, this paper introduces a new decomposition, not of the flux vector, but of the hyperbolic-flux Jacobian, termed a FJD. Generalizing and encompassing flux-vector and FDSs, as summarized in Section 4.2, this decomposition expresses the hyperbolic-flux Jacobian as the sum of $L$ contributions in the form

$$\frac{\partial f_j}{\partial q} = \sum_{\ell=1}^{L} \alpha_\ell A_{\ell j} \;\Rightarrow\; \frac{\partial f_j}{\partial x_j} = \sum_{\ell=1}^{L} \alpha_\ell A_{\ell j} \frac{\partial q}{\partial x_j} \tag{21}$$

where $\alpha_\ell$ denotes a linear-combination function, possibly depending upon $q$, $A_{\ell j}$ corresponds to a flux-Jacobian matrix component such that the matrix $A_{\ell j} n_j$ has uniform-sign eigenvalues within a conical region spanned by a unit vector $\mathbf{n}$, with components $n_j$, within the flow space.

   An integral average of the hyperbolic flux divergence $\partial f_j / \partial x_j$ as expressed through decomposition (21) becomes

$$\int_{\hat{\Omega}} \hat{w} \frac{\partial f_j}{\partial x_j} \, d\Omega = \int_{\hat{\Omega}} \sum_{\ell=1}^{L} \hat{w} \alpha_\ell A_{\ell j} \frac{\partial q}{\partial x_j} \, d\Omega \tag{22}$$

By comparison, the flux $f_j^C$ is defined by way of an upstream-bias integral average as

$$\int_{\hat{\Omega}} \hat{w} \frac{\partial f_j^C}{\partial x_j} \, d\Omega \equiv \int_{\hat{\Omega}} \sum_{\ell=1}^{L} (\hat{w} + \psi \, \delta_\ell \hat{w}) \alpha_\ell A_{\ell j} \frac{\partial q}{\partial x_j} \, d\Omega \tag{23}$$

where the RHS integral provides an upstream bias for each matrix component within the FJD in (21).

   As documented in Reference [18], the positive $\psi$ in (23), $0 < \psi \leqslant 1$, stands for an 'upstream-bias' controller, which automatically adjusts the amount of induced upstream-bias diffusion, depending on local solution non-smoothness, with $\psi = 0$ corresponding to a centred discretization, on any grid, and $\psi = 1$ generating a fully upwind formulation. In regions of solutions smoothness, $\psi$ decreases to a minimum for accuracy, whereas in the neighbourhood of shocks, $\psi$ increases to a maximum for an essentially non-oscillatory stable shock capturing.

   The expression $\delta_\ell \hat{w}$ denotes a directional variation of the test function $\hat{w}$ along an upstream-bias principal direction, the axis of a conical region within the flow space, as

$$\delta_\ell \hat{w} \equiv \frac{\partial \hat{w}}{\partial x_j} \delta_\ell x_j = \frac{\partial \hat{w}}{\partial x_j} a_{j\ell} \varepsilon, \quad \delta_\ell x_j \equiv a_{j\ell} \varepsilon \tag{24}$$

In this expansion, $\varepsilon$ denotes a reference length and $a_{j\ell}$, $1 \leqslant j \leqslant 3$, denotes the $j$th component of the unit vector $\mathbf{a}_\ell$ in the direction of the '$\ell$th' upstream-bias principal direction. This variation induces the appropriate upstream bias for the test function $\hat{w}$ for each '$\ell$' component within (23). Depending on the physical significance, magnitude and algebraic sign of the eigenvalues of $A_{\ell j} n_j$, the variation $\delta_\ell \hat{w}$ can vanish or become algebraically positive or negative, which corresponds to an upstream bias, respectively, in the negative or positive sense of the axis of each conical region.

An integration by parts of the RHS of (23) and subsequent comparison with its LHS generates the following expression for the divergence of the characteristics flux $f_j^C$:

$$\frac{\partial f_j^C}{\partial x_j} = \frac{\partial f_j}{\partial x_j} - \frac{\partial}{\partial x_i} \left( \varepsilon \psi \sum_{\ell=1}^{L} a_{i\ell} \alpha_\ell A_{\ell j} \frac{\partial q}{\partial x_j} \right) \tag{25}$$

This expression exhibits an upstream-bias artificial diffusion, in the form of a second-order differential expression with associated upstream-bias matrix

$$\mathscr{A} \equiv n_i \left( \sum_{\ell=1}^{L} a_{i\ell} \alpha_\ell A_{\ell j} \right) n_j \tag{26}$$

where $n_i$ indicates the $i$th direction cosine of a unit vector $\mathbf{n}$ along an arbitrary wave-propagation direction, as depicted in Figure 1. For physical consistency of the upstream bias in (23), (25) as well as associated mathematical stability of the corresponding second-order differential expression, all the eigenvalues of this upstream-bias matrix must be positive at every flow-field point and for any wave-propagation direction $\mathbf{n}$ [21, 22]. Implying a consistent upstream bias along all directions radiating from any flow field point, this requirement becomes a fundamental upstream-bias stability condition.

On the basis of these developments, the procedure for generating a specific characteristics bias involves the following steps. Firstly, for the given hyperbolic flux, a FJD (22) is developed, as guided by a characteristics analysis analogous to the one in Section 3. Secondly, specific constraints on the FJD parameters $\alpha_\ell$ and direction-cosine components $a_{i\ell}$ are established, as directed by the upstream-bias stability condition. Section 5 shows how this procedure generates a characteristics-bias flux for the hyperbolic flux in the Euler and Navier–Stokes equations.

## 4.2. Incorporation of FVS and FDSs

The FJD procedure generalizes and encompasses traditional FVS and FDS formulations. Consider the representative flux-vector splitting (FVS) of the Euler flux as

$$f_j(q) = f_j^+(q) + f_j^-(q) \tag{27}$$

where the Jacobian matrices of $(\partial f_j^+/\partial q)n_j$ and $(\partial f_j^-/\partial q)n_j$, respectively, possess non-negative and non-positive eigenvalues within a conical region with axis with direction cosines $n_j$, $1 \leqslant j \leqslant 3$. The FJD expression (21) encompasses (27) with $L = 2$ as

$$\sum_{\ell=1}^{L} \alpha_\ell A_{\ell j} = \frac{\partial f_j^+}{\partial q} + \frac{\partial f_j^-}{\partial q}, \quad \alpha_1 = 1, \quad \alpha_2 = 1 \tag{28}$$

The corresponding characteristics-bias flux divergence for this representative FVS accrues from (25) as

$$\frac{\partial f_j^C}{\partial x_j} = \frac{\partial f_j}{\partial x_j} - \frac{\partial}{\partial x_i} \left( \varepsilon \psi \left( a_i^+ \frac{\partial f_j^+}{\partial x_j} - a_i^- \frac{\partial f_j^-}{\partial x_j} \right) \right) \tag{29}$$

which generalizes in the continuum the traditional numerical flux formulae for FVS constructions. The associated upstream-bias matrix $\mathscr{A}$ is

$$\mathscr{A} = \sum_{i,j=1}^{3} n_i \left( a_i^+ \frac{\partial f_j^+}{\partial q} + a_i^- \frac{\partial f_j^-}{\partial q} \right) n_j \tag{30}$$

where the flux components $f_j^+$ and $f_j^-$ as well as the direction cosines $a_i^+$ and $a_i^-$, frequently $a_i^- = -a_i^+$, should be chosen to satisfy the upstream-bias stability condition on this matrix.

Consider next a representative FDS development, where the inviscid flux Jacobian of $f_j$ is 'split' as

$$\frac{\partial f_j}{\partial q} = X_{\underline{j}} \Lambda_j^+ X_{\underline{j}}^{-1} + X_{\underline{j}} \Lambda_j^- X_{\underline{j}}^{-1} \tag{31}$$

where $X_{\underline{j}}$ and $\Lambda_j = \Lambda_j^+ + \Lambda_j^-$ denote the right eigenvector matrix and eigenvalue diagonal matrix of the Jacobian, all evaluated at special average values of $q$, with $\Lambda_j^+$ and $\Lambda_j^-$, respectively, containing non-negative and non-positive eigenvalues. The matrices at the RHS of (31), therefore, will, respectively, possess non-negative and non-positive eigenvalues. The FJD expression (21) encompasses (31) with $L = 2$ as

$$\sum_{\ell=1}^{L} \alpha_\ell A_{\ell j} = X_{\underline{j}} \Lambda_j^+ X_{\underline{j}}^{-1} + X_{\underline{j}} \Lambda_j^- X_{\underline{j}}^{-1}, \quad \alpha_1 = 1, \ \alpha_2 = 1 \tag{32}$$

The corresponding characteristics-bias divergence for this formulation accrues from (25) as

$$\frac{\partial f_j^{\mathrm{C}}}{\partial x_j} = \frac{\partial f_j}{\partial x_j} - \frac{\partial}{\partial x_i} \left( \varepsilon \psi \left( a_i^+ \sum_{j=1}^{3} (X_{\underline{j}} \Lambda_j^+ X_{\underline{j}}^{-1}) + a_i^- \sum_{j=1}^{3} (X_{\underline{j}} \Lambda_j^- X_{\underline{j}}^{-1}) \right) \frac{\partial q}{\partial x_j} \right)$$

$$= \frac{\partial f_j}{\partial x_j} - \frac{\partial}{\partial x_i} \left( \varepsilon \psi \sum_{j=1}^{3} X_{\underline{j}} (a_i^+ \Lambda_j^+ + a_i^- \Lambda_j^-) X_{\underline{j}}^{-1} \frac{\partial q}{\partial x_j} \right) \tag{33}$$

which generalizes in the continuum the traditional numerical flux formulae for FDS constructions. The associated upstream-bias matrix $\mathscr{A}$ is

$$\mathscr{A} = \sum_{i,j=1}^{3} n_i X_{\underline{j}} (a_i^+ \Lambda_j^+ + a_i^- \Lambda_j^-) X_{\underline{j}}^{-1} n_j \tag{34}$$

where the eigenvalue-matrix components $\Lambda_j^+$ and $\Lambda_j^-$ as well as the direction cosines $a_i^+$ and $a_i^-$, frequently $a_i^- = -a_i^+$, should be chosen to satisfy the upstream-bias stability condition on this matrix.

## 5. ACOUSTICS–CONVECTION CHARACTERISTICS EULER FLUX

As a guiding principle in formulating this particular Euler FJD, the form of the eventual characteristics-bias flux divergence should minimally depart from the form of the Euler flux

divergence, both for efficiency of implementation and accuracy of numerical computations. The acoustics–convection FJD consists of components that genuinely model the physics of multi-dimensional acoustics and convection. These components lead to an algorithm that combines the computational simplicity of FVS with the accuracy and stability of FDS and also feature eigenvalues with uniform algebraic sign. This formulation eliminates an unstable linear-dependence problem in steady low-Mach-number flows and satisfies by design the upstream-bias stability condition. As the Mach number increases, the formulation smoothly approaches and then becomes an upstream-bias approximation of the entire flux divergence, along the principal streamline direction.

### 5.1. Convection and pressure-gradient components

For supersonic flows, the Euler eigenvalues (15) associated with the Jacobian $\partial f_j/\partial q$ all have the same algebraic sign within a streamline wedge region so that within this region the entire flux divergence $\partial f_j/\partial x_j$ can be upstream approximated along the streamline principal direction. For subsonic flows these eigenvalues have mixed algebraic sign and an upstream approximation for the flux divergence along one single direction remains inconsistent with the two-way propagation of acoustic waves. Since for subsonic flows it is the pressure gradient in the momentum equation that induces mixed-sign eigenvalues, by suitably decreasing the contribution from this gradient the resulting flux-Jacobian eigenvalues all have the same algebraic sign within a streamline wedge region and the resulting convection flux divergence can then be upstream approximated along one single direction.

Following this consideration, the flux Jacobian $\partial f_j/\partial q$ is decomposed as

$$\frac{\partial f_j}{\partial q} = \left[ \frac{\partial f_j^q}{\partial q} + \beta \frac{\partial f_j^p}{\partial q} \right] + (1 - \beta) \left[ \frac{\partial f_j^p}{\partial q} \right] \tag{35}$$

where $f_j^q$ and $f_j^p$, respectively, denote the convection and pressure flux components

$$f_j^q(q) \equiv \left\{ \begin{array}{c} m_j \\ \dfrac{m_j}{\rho} m_1 \\ \dfrac{m_j}{\rho} m_2 \\ \dfrac{m_j}{\rho}(E + p) \end{array} \right\} = \frac{m_j}{\rho} \cdot \left\{ \begin{array}{c} \rho \\ m_1 \\ m_2 \\ E + p \end{array} \right\}, \quad f_j^p(q) \equiv \left\{ \begin{array}{c} 0 \\ p\delta_1^j \\ p\delta_2^j \\ 0 \end{array} \right\} \tag{36}$$

Of the four eigenvalues of the pressure Jacobian $(\partial f_j^p/\partial q)n_j$, three of them identically vanish and the fourth has been exactly determined as $\lambda_4^p = -u_j n_j p_E$. Remaining independent of the speed of sound $c$, this eigenvalue becomes negligible for low Mach numbers. Considering that all of these pressure eigenvalues vanish in these conditions, an upstream-bias approximation of the isolated pressure gradient is unnecessary, for it would not represent acoustic or any other propagation.

Since the eigenvalues of a matrix continuously depend on the matrix coefficients [26] and since for $\beta = 0$ the eigenvalues of the Jacobian matrix $[(\partial f_j^q/\partial q) + \beta(\partial f_j^p/\partial q)]n_j$ all display the same algebraic sign within a conical region with axis with components $n_j$, it is possible

to establish a Mach-number-dependent positive increasing function $\beta = \beta(M)$, $0 \leqslant \beta \leqslant 1$, so that the eigenvalues of this Jacobian matrix retain the same sign, as $\beta$ increases towards 1 for increasing subsonic $M$. With such a formulation, this Jacobian matrix can be upstream biased in the streamline direction while it approaches and then becomes the complete Jacobian matrix $(\partial f_j / \partial q) n_j$ for $M > 1$. In view of (14), for vanishing Mach number the eigenvalues of $[(\partial f_j^q / \partial q) + \beta(\partial f_j^p / \partial q)] n_j$ can all keep the same algebraic sign, however, when $\beta = 0$, which eliminates the speed-of-sound $\pm c$ contribution from (14). Forcing the resulting eigenvalues to vanish, this elimination obliterates the acoustic components so that an upstream bias approximation of $[(\partial f_j^q / \partial q) + \beta(\partial f_j^p / \partial q)]$ in these conditions would inaccurately model the contributions from acoustic waves. It follows that for low Mach numbers, an alternative decomposition of the full Jacobian must be devised to model accurately the acoustic waves.

### 5.2. Acoustics components

For arbitrary Mach numbers and corresponding dependent variables $\rho$, $m_1$, $m_2$ and $E$, the Euler flux Jacobians can also be decomposed as

$$\frac{\partial f_j}{\partial q} = \frac{\partial f_j^q}{\partial q} + \frac{\partial f_j^p}{\partial q} = \frac{\partial f_j^q}{\partial q} + A_j^a + A_j^{nc} \tag{37}$$

where the matrices $A_j^a$ and $A_j^{nc}$ are

$$A_j^{nc} \equiv \begin{pmatrix} 0 & -\delta_1^j & -\delta_2^j & 0 \\ 0 & p_{m_1}\delta_1^j & p_{m_2}\delta_1^j & 0 \\ 0 & p_{m_1}\delta_2^j & p_{m_2}\delta_2^j & 0 \\ 0 & -\dfrac{c^2 - p_\rho}{p_E}\delta_1^j & -\dfrac{c^2 - p_\rho}{p_E}\delta_1^j & 0 \end{pmatrix} \tag{38}$$

$$A_j^a \equiv \begin{pmatrix} 0 & \delta_1^j & \delta_2^j & 0 \\ p_\rho\delta_1^j & 0 & 0 & p_E\delta_1^j \\ p_\rho\delta_2^j & 0 & 0 & p_E\delta_2^j \\ 0 & \dfrac{c^2 - p_\rho}{p_E}\delta_1^j & \dfrac{c^2 - p_\rho}{p_E}\delta_2^j & 0 \end{pmatrix} \tag{39}$$

Note, in particular, that no flux component of $f_j(q)$ exists, of which the Jacobian equals $A_j^a$, the system matrix of the acoustics equations. This matrix also becomes the entire flux Jacobian at the LHS of (37) for vanishing $M$. In these conditions, as shown by the first and fourth rows in $A_j^a$, the continuity and energy equations become linearly dependent; this linear dependence provides an additional explanation for the widely reported convergence difficulties experienced by numerous Euler solvers for low Mach numbers. Physically, this linear dependence signifies that, for low Mach numbers, an inviscid flow becomes isentropic, which obviates the need

of an energy equation to determine $\rho$, $m_1$, $m_2$ and $E$. The formulation detailed in this paper eliminates this linear dependence within the developed upstream-bias algorithm.

The eigenvalues of the matrix $A_j^{nc} n_j$ have been determined in closed form as

$$\lambda_{1,3}^{nc} = 0, \quad \lambda_4^{nc} = -cMp_E v_j n_j \tag{40}$$

which become infinitesimal for vanishing $M$. The matrix $A_j^{nc}$ can be termed a 'non-linear coupling' matrix, for it completes the non-linear coupling between convection and acoustics within (37) so that the Euler eigenvalues can correspond to the sum of convection and acoustic speeds. Since the matrix $A_j^a$ will be used in the upstream-bias formulation for small Mach numbers only and considering that the eigenvalues in (40) vanish both for these Mach numbers and for **n** pointing in the crossflow direction, for which $v_j n_j = 0$, no need exists to involve $A_j^{nc}$ in the upstream-bias approximation of the Euler flux Jacobian.

Having been exactly determined in closed form as

$$\lambda_{1,2}^a = 0, \quad \lambda_{3,4}^a = \pm c \tag{41}$$

the non-vanishing eigenvalues of $A_j^a n_j$ equal the speed of sound and remain independent of the propagation vector **n**, which signifies isotropic propagation and confirms that the matrix $A_j^a$, is the 'acoustics' matrix. This matrix, therefore, can be used for an upstream-bias approximation of the Euler and Navier–Stokes equations in the low Mach-number regime, within the streamline region, and for any Mach number, within the crossflow region.

For any two mutually perpendicular unit vectors $\mathbf{a} = (a_1, a_2)$ and $\mathbf{a}^N = (a_1^N, a_2^N)$ within a 2-D flow, along with implied summation on repeated indices, the acoustics component within the Euler flux divergence can be further decomposed as

$$A_j^a \frac{\partial q}{\partial x_j} = A_j^a a_j a_k \frac{\partial q}{\partial x_k} + A_j^a a_j^N a_k^N \frac{\partial q}{\partial x_k} \tag{42}$$

For **a** parallel to **u**, this expression corresponds to a decomposition of the Euler acoustics component into streamline and crossflow acoustics components. Two eigenvalues of each component vanish; the remaining eigenvalues of these separate streamline and crossflow components have been determined as

$$\lambda_{3,4}^s = \pm c a_j n_j, \quad \lambda_{3,4}^N = \pm c a_j^N n_j \tag{43}$$

which shows that the streamline eigenvalues vanish in the crossflow direction, for $a_j n_j = 0$ with $n_j = a_j^N$, and the crossflow eigenvalues vanish in the streamline direction, for $a_j^N n_j = 0$ with $n_j = a_j$; this observation, in particular, indicates that the streamline acoustics component can induce no upstream bias in the crossflow direction and, analogously, the crossflow acoustics component can induce no upstream bias in the streamline direction.

The two non-vanishing eigenvalues associated with the entire acoustics component at the LHS of (42), but as expressed as the RHS combination of streamline and crossflow components have then been determined as

$$\lambda_{3,4}^a = c((a_j n_j)^2 + (a_j^N n_j)^2)^{1/2}, \quad (a_j n_j)^2 + (a_j^N n_j)^2 = 1 \tag{44}$$

which shows that the square of the acoustic eigenvalues (41) equals the sum of the square of the streamline and crossflow acoustic eigenvalues (43). For **a** and $\mathbf{a}^N$, respectively, pointing in

the streamline and crossflow directions, the Euler flux divergence can then be decomposed as

$$\frac{\partial f_j(q)}{\partial x_j} = A_j^a a_j a_k \frac{\partial q}{\partial x_k} + A_j^a a_j^N a_k^N \frac{\partial q}{\partial x_k} + \frac{\partial f_j^q}{\partial x_j} + A_j^{nc} \frac{\partial q}{\partial x_j} \tag{45}$$

Despite its zero eigenvalues, the matrix $A_j^a a_j$ has been found to feature a complete set of eigenvectors $X$ and thus possesses the similarity-transformation form

$$A_j^a a_j = X \Lambda^a X^{-1} = X \Lambda^{a+} X^{-1} + X \Lambda^{a-} X^{-1}, \quad \Lambda^a = \Lambda^{a+} + \Lambda^{a-} \tag{46}$$

where the diagonal matrix $\Lambda^a$ contains eigenvalues (41) and the diagonal matrices $\Lambda^{a+}$ and $\Lambda^{a-}$, respectively, contain non-negative and non-positive contributions to these eigenvalues. The matrices $X \Lambda^{a+} X^{-1}$ and $X \Lambda^{a-} X^{-1}$, respectively, correspond to the 'forward' and 'backward' acoustic-propagation matrix components of $A_j^a a_j$. Based on these matrices, a bi-modal upstream-bias approximation of $A_j^a a_j$, follows from instituting a forward and a backward upstream-bias approximation, respectively, for the forward- and backward-propagation matrices in (46). Results similar to (46) then readily follow by replacing **a** with $\mathbf{a}^N$. This bi-modal approximation also depends on the specific choices for the diagonal matrices $\Lambda^{a+}$ and $\Lambda^{a-}$, with different choices associated to different levels of accuracy and induced dissipation. The following choices for these matrices

$$\Lambda^{a+} \equiv \frac{1}{2} \begin{pmatrix} 2c & 0 & 0 & 0 \\ 0 & 0 & 0 & 0 \\ 0 & 0 & c & 0 \\ 0 & 0 & 0 & c \end{pmatrix}, \quad \Lambda^{a-} \equiv -\frac{1}{2} \begin{pmatrix} 0 & 0 & 0 & 0 \\ 0 & 2c & 0 & 0 \\ 0 & 0 & c & 0 \\ 0 & 0 & 0 & c \end{pmatrix} \tag{47}$$

directly yield particularly simple forms for both the non-negative-eigenvalue matrices

$$|A_j^a a_j| \equiv X(\Lambda^{a+} - \Lambda^{a-})X^{-1} = cI, \quad |A_j^a a_j^N| \equiv X_N(\Lambda^{a+} - \Lambda^{a-})X_N^{-1} = cI \tag{48}$$

and the associated matrix products

$$|A_j^a a_j| a_k \frac{\partial q}{\partial x_k} = cI a_k \frac{\partial q}{\partial x_k}, \quad |A_j^a a_j^N| a_k^N \frac{\partial q}{\partial x_k} = cI a_k^N \frac{\partial q}{\partial x_k} \tag{49}$$

with $I$ denoting the identity matrix. The matrices in (48), respectively, correspond to the absolute streamline and crossflow acoustics matrices.

The developments in this section, on the one hand, show that decomposition (45) leads to a physically consistent representation of acoustic propagation. On the other hand, in view of (49), an upstream-bias representation of this decomposition induces more diffusion than (35) for increasing Mach number.

### 5.3. Acoustics–convection flux-divergence decomposition

The developments in the previous two sections have established decompositions (35) and (45). The first decomposition induces less diffusion than (45), for increasing Mach number, but it cannot represent acoustic propagation for low subsonic Mach numbers; the second consistently

models acoustic propagation, but induces more diffusion than (35) for increasing Mach number. An acoustics–convection flux-divergence decomposition that not only induces minimal diffusion, but also models acoustic propagation is thus established as a linear combination of (35) and (45), with linear combination parameter $\alpha$ and $0 \leqslant \alpha, \beta \leqslant 1$

$$\frac{\partial f_j(q)}{\partial x_j} = \alpha(X\Lambda^{a+}X^{-1} + X\Lambda^{a-}X^{-1})a_k \frac{\partial q}{\partial x_k} + \alpha(X_N\Lambda^{a+}X_N^{-1} + X_N\Lambda^{a-}X_N^{-1})a_k^N \frac{\partial q}{\partial x_k}$$

$$+ \alpha A_j^{nc} \frac{\partial q}{\partial x_j} + \left[ \frac{\partial f_j^q}{\partial x_j} + (1-\alpha)\beta \frac{\partial f_j^p}{\partial x_j} \right] + (1-\alpha)(1-\beta) \frac{\partial f_j^p}{\partial x_j} \qquad (50)$$

Owing to the simplifying parameter $\delta \equiv \beta(1-\alpha)$ and introducing the crossflow acoustic upstream parameter $\alpha^N$, with $0 \leqslant \delta$, $\alpha^N \leqslant 1$, the final form of the acoustics–convection flux-divergence decomposition becomes

$$\frac{\partial f_j(q)}{\partial x_j} = \alpha(X\Lambda^{a+}X^{-1} + X\Lambda^{a-}X^{-1})a_k \frac{\partial q}{\partial x_k} + \alpha^N(X_N\Lambda^{a+}X_N^{-1} + X_N\Lambda^{a-}X_N^{-1})a_k^N \frac{\partial q}{\partial x_k}$$

$$+ \left[ \frac{\partial f_j^q}{\partial x_j} + \delta \frac{\partial f_j^p}{\partial x_j} \right] + (1-\alpha-\delta) \frac{\partial f_j^p}{\partial x_j} + \alpha A_j^{nc} \frac{\partial q}{\partial x_j} + (\alpha - \alpha^N)A_j^a a_j^N a_k^N \frac{\partial q}{\partial x_k} \quad (51)$$

The weights $\alpha$ and $\alpha^N$, respectively, for the streamline and crossflow acoustic components in this expression are different from each other because the streamline and crossflow characteristic velocity components remain different from each other, following the Euler eigenvalues (16). For increasing Mach number, furthermore, the pressure gradient term $\delta(\partial f_j^p / \partial x_j)$ in this decomposition also contributes to the streamline acoustic upstream bias. These considerations indicate that the magnitudes of acoustic upstream bias for (51) along the streamline and crossflow directions will have to differ from each other for varying $M$, a 'differential' upstream bias that can be instituted through the distinct weights $\alpha$ and $\alpha^N$ on the streamline and crossflow acoustic components. With respect to the expression $[(\partial f_j^q / \partial x_j) + \delta(\partial f_j^p / \partial x_j)]$, this is enclosed in square brackets and counted as one single term because all the streamline eigenvalues of the associated Jacobian display the same algebraic sign.

A characteristics-bias formulation from decomposition (51) is obtained following the two principles of minimal upstream dissipation and consistent infinite-directional upstream bias. According to these principles, the developments in the following sections show that for $M = 0$, the functions $\alpha$ and $\alpha^N$ equal 1, whereas the function $\delta$ equals 0; for increasing $M$, $\alpha$ rapidly decreases and vanishes, $\delta$ rapidly increases and then identically equals 1, for supersonic flows, and $\alpha^N$ monotonically decreases. Based on these principles, furthermore, it is unnecessary to establish an upstream-bias formulation for the last three terms in decomposition (51) for the following reasons. With reference to the first of these three terms, the preceding term between square brackets will already contribute an upstream-bias representation for the pressure gradient; additionally, the coefficient $(1-\alpha-\delta)$ of this term vanishes for acoustic and supersonic flows and three out of four eigenvalues of the Jacobian of this term identically vanish, as discussed in Section 5.1 after Equation (36). With respect to the second of these three terms,

an upstream bias of this term would essentially add only algebraic complexity to the formulation, for its coefficient $\alpha$ rapidly decreases and then vanishes for supersonic and high subsonic Mach numbers; additionally, three out of four eigenvalues of the Jacobian of this term vanish, as discussed in Section 5.2 after Equation (40), and the product of $\alpha$ and the remaining fourth eigenvalue remains negligible for $\alpha > 0$. Concerning the third of these three terms, of the four eigenvalues of its Jacobian matrix, two identically vanish and the remaining two vanish in the streamline direction, implying no upstream bias in this direction, as discussed in Section 5.2 after results (43); additionally, an upstream-bias formulation for this term would obliterate the acoustic crossflow upstream bias induced by the $\alpha^N(X_N \Lambda^{a+} X_N^{-1} + X_N \Lambda^{a-} X_N^{-1})$ matrix in (51); as Section 6.4 shows, this crossflow acoustics dissipation remains essential for stability of the eventual upstream-bias formulation. Based on all these considerations, the following sections establish a computationally efficient characteristics-bias flux for the Euler flux divergence.

## 5.4. Multi-dimensional characteristics Euler flux

With reference to (25), given the physical significance of the terms in decomposition (51) and algebraic signs of the corresponding eigenvalues, the associated principal direction unit vectors for these terms are

$$\mathbf{a}_1 = -\mathbf{a}_2 = \mathbf{a}_5 = \mathbf{a}, \quad \mathbf{a}_3 = -\mathbf{a}_4 = \mathbf{a}^N, \quad \mathbf{a}_6 = \mathbf{a}_7 = \mathbf{a}_8 = \mathbf{0} \tag{52}$$

At each flow-field point, $\mathbf{a}$ and $\mathbf{a}^N$ remain, respectively, parallel and perpendicular to the local velocity, with $\mathbf{a}^N$ obtained by a 90°-degree anti-clockwise rotation of $\mathbf{a}$.

Based on (48), (49), (51), (52), the general upstream-bias expression (25) directly yields the acoustics–convection characteristics flux divergence

$$\frac{\partial f_j^C}{\partial x_j} = \frac{\partial f_j}{\partial x_j} - \frac{\partial}{\partial x_i}\left[\varepsilon\psi\left(c(\alpha a_i a_j + \alpha^N a_i^N a_j^N)\frac{\partial q}{\partial x_j} + a_i\frac{\partial f_j^q}{\partial x_j} + a_i\delta\frac{\partial f_j^p}{\partial x_j}\right)\right] \tag{53}$$

In this result, the expressions $(c\alpha a_i a_j(\partial q/\partial x_j) + a_i(\partial f_j^q/\partial x_j) + a_i\delta(\partial f_j^p/\partial x_j))$ and $(c\alpha^N a_i^N a_j^N(\partial q/\partial x_j))$ determine the upstream biases within, respectively, the streamline and cross-flow wave propagation regions. These two expressions combined then induce a consistent upwind bias along all wave propagation regions. As $M$ increases, the streamline acoustics upstream bias derives more from the pressure gradient and less from the acoustics matrix, so that for supersonic flows the streamline upstream bias entirely results from the physical Euler flux divergence. The operation count for expression (53) is then comparable to that of an FVS formulation. The terms in this expression, furthermore, directly correspond to the physics of acoustics and convection. Expression (53) determines $f_i^C$ itself, up to an arbitrary divergence-free vector, as

$$f_i^C = f_i(q) - \varepsilon\psi\left[c(\alpha a_i a_j + \alpha^N a_i^N a_j^N)\frac{\partial q}{\partial x_j} + a_i\frac{\partial f_j^q}{\partial x_j} + a_i\delta\frac{\partial f_j^p}{\partial x_j}\right] \tag{54}$$

According to this result, the intrinsic multi-dimensionality of each component $f_i^C$ derives from its dependence upon the entire divergence of $f_j^q$ and $f_j^p$. For vanishing Mach numbers, $\alpha$ and $\alpha^N$ will approach 1 whereas $\delta$ will approach 0. Under these conditions, (53)

reduces to

$$\frac{\partial f_j^{\mathrm{C}}}{\partial x_j} = \frac{\partial f_j}{\partial x_j} - \frac{\partial}{\partial x_i}\left[\varepsilon\psi\left(c\,\frac{\partial q}{\partial x_i} + a_i\,\frac{\partial f_j^q}{\partial x_j}\right)\right] \tag{55}$$

which essentially induces only an acoustics upstream bias. Note that this bias becomes independent of specific propagation directions, for it no longer depends on $(\alpha a_i a_j + \alpha^N a_i^N a_j^N)$. This bias, therefore, becomes isotropic, in harmony with the isotropic propagation of acoustic waves. Observe, moreover, that the components within $\partial f_j^{\mathrm{C}}/\partial x_j$ remain linearly independent of one another, which avoids the linear-dependence instability in the steady low Mach-number Euler equations. For supersonic flows, $\alpha = 0$ and $\delta = 1$ and (53) thus becomes

$$\frac{\partial f_j^{\mathrm{C}}}{\partial x_j} = \frac{\partial f_j}{\partial x_j} - \frac{\partial}{\partial x_i}\left[\varepsilon\psi\left(c\alpha^N a_i^N a_j^N\,\frac{\partial q}{\partial x_j} + a_i\,\frac{\partial f_j}{\partial x_j}\right)\right] \tag{56}$$

which depends not only on the entire divergence of the Euler inviscid flux vector, but also on the crossflow component of the absolute acoustics matrix. Section 6.4 shows this matrix is needed because even for a supersonic flow, the Euler flux Jacobian eigenvalues $\lambda_{3,4}^E$ in (16) remain of mixed algebraic sign within a conical region about the crossflow direction, due to acoustic propagation.

## 6. CONSISTENT INFINITE DIRECTIONAL UPSTREAM BIAS

In Jacobian form, expression (53) becomes

$$\frac{\partial f_j^{\mathrm{C}}}{\partial x_j} = \frac{\partial f_j}{\partial x_j} - \frac{\partial}{\partial x_i}\left[\varepsilon\psi\left(c(\alpha a_i a_j + \alpha^N a_i^N a_j^N)I + a_i\,\frac{\partial f_j^q}{\partial q} + a_i\delta\,\frac{\partial f_j^p}{\partial q}\right)\frac{\partial q}{\partial x_j}\right] \tag{57}$$

For 2-D flows, expression (53) and this upstream-bias expression essentially depend upon the five upstream-bias functions $a_1, a_2, \alpha, \delta, \alpha^N$. In order to ensure physical consistency, these functions are determined by imposing on (57) the stringent stability requirement that it should induce an upstream-bias diffusion not just along the principal streamline and crossflow upstream directions, but along all directions $\mathbf{n} = (n_1, n_2)$ radiating from any flow-field point. This is a demanding stability condition on the FJD matrix (26), which is satisfied when all the eigenvalues of the acoustics–convection upstream-bias matrix

$$\mathscr{A} \equiv n_i\left(c(\alpha a_i a_j + \alpha^N a_i^N a_j^N)I + a_i\,\frac{\partial f_j^q}{\partial q} + a_i\delta\,\frac{\partial f_j^p}{\partial q}\right)n_j \tag{58}$$

remain positive for all $M$ and propagation directions $\mathbf{n}$.

Despite the formidable non-linear algebraic complexity of $\mathscr{A}$, all of its eigenvalues have been analytically determined exactly in closed form. Dividing through the speed of sound $c$, the non-dimensional form of these eigenvalues is

$$\lambda_{1,2} = n_i(\alpha a_i a_j + \alpha^N a_i^N a_j^N)n_j + n_i a_i v_j n_j M$$

$$\lambda_{3,4} = n_i(\alpha a_i a_j + \alpha^N a_i^N a_j^N)n_j + n_i a_i \left(1 + \frac{1-\delta}{2} p_E\right) v_j n_j M \pm n_i a_i \sqrt{\left(\frac{1-\delta}{2} p_E v_j n_j M\right)^2 + \delta} \quad (59)$$

where $v_j$ denotes the $j$th direction cosine of a unit vector $\mathbf{v}$ parallel to the local velocity $\mathbf{u}$. Note that for both $\mathbf{a} = \mathbf{v}$ and $\mathbf{n} = \mathbf{v}$, the functions $\alpha$ and $\delta$ within (59) determine the corresponding streamline upstream-bias eigenvalues, already established in Reference [18]

$$\lambda_{1,2} = \alpha + M, \quad \lambda_{3,4} = \alpha + \left(1 + \frac{1-\delta}{2} p_E\right)M \pm \sqrt{\left(\frac{1-\delta}{2} p_E M\right)^2 + \delta} \quad (60)$$

Rather than prescribing some expressions for $\alpha$ and $\delta$ and accepting the resulting variations for these eigenvalues, physically consistent expressions for the streamline upstream-bias eigenvalues are instead prescribed and the corresponding functions for $\alpha$ and $\delta$ determined.

### 6.1. Conditions on upstream-bias functions and eigenvalues

Eigenvalues (59) are expressed as

$$\lambda_{1,4} = \lambda_{1,4}(M, \mathbf{n}) \quad (61)$$

to stress their dependence upon both $M$ and $\mathbf{n}$. The five conditions for the determination of the five functions $a_1, a_2, \alpha, \delta, \alpha^N$ are

$$a_1^2 + a_2^2 = 1, \quad \lambda_{1,2}(M, \mathbf{n}) \geqslant 0, \quad \lambda_1(M, \mathbf{v}) = \lambda_1, \quad \lambda_4(M, \mathbf{v}) = \lambda_4, \quad \lambda_{3,4}(M, \mathbf{n}) \geqslant 0 \quad (62)$$

where $\lambda_1$ and $\lambda_4$ now denote prescribed streamline upstream-bias eigenvalues. The first condition stipulates $\mathbf{a}$ as a unit vector and with the second condition it determines both $\mathbf{a}$ and $\mathbf{a}^N$, for $\mathbf{a}$ and $\mathbf{a}^N$ are mutually perpendicular. In particular, these two conditions theoretically confirm that the unit vectors $\mathbf{a}$ and $\mathbf{a}^N$, respectively, point along the streamline and crossflow directions. The third and fourth conditions stipulate that the streamline upstream-bias eigenvalues must equal prescribed eigenvalues, which leads to $\alpha$ and $\delta$. For the determined $\mathbf{a}$, $\mathbf{a}^N$, $\alpha$ and $\delta$, the fifth condition then establishes $\alpha^N$.

### 6.2. Streamline eigenvalue $\lambda_4$

This eigenvalue will correlate with the absolute Euler eigenvalue $|M-1|$. As a consequence, $\lambda_4$ will vary between 1 and $1-M$ for $0 \leqslant M \leqslant 1 - \varepsilon_M$ and smoothly shift from $1-M$ to $M-1$ within the transonic layer $1 - \varepsilon_M \leqslant M \leqslant 1 + \varepsilon_M$, where $\varepsilon_M$ denotes a transonic-layer parameter; in this work $\varepsilon_M = \frac{1}{5}$. One expression for $\lambda_4$ that remains smooth and meets these requirements

is the composite spline

$$\lambda_4(M) \equiv \begin{cases} 1 - M, & 0 \leqslant M \leqslant 1 - \varepsilon_M \\ \dfrac{(M-1)^2}{2\varepsilon_M} + \dfrac{\varepsilon_M}{2}, & 1 - \varepsilon_M < M < 1 + \varepsilon_M \\ M - 1, & 1 + \varepsilon_M \leqslant M \end{cases} \tag{63}$$

### 6.3. Streamline eigenvalue $\lambda_1$

This eigenvalue correlates with the non-dimensional Euler eigenvalue $M$, but it too has to equal 1 for $M = 0$; it then must coincide with $M$ for $M > 1$ and also remain greater than $\lambda_4$, as expressed through (63), for consistency with the Euler eigenvalues (15) and complete separation of eigenvalues (59). This condition in particular implies $\lambda_1 \geqslant \frac{1}{2}$. It thus follows that $\lambda_1$ will vary between 1 and $M$ for $0 \leqslant M \leqslant \frac{1}{2} + \varepsilon_M$. An expression for $\lambda_1 = \lambda_1(M)$ that remains smooth and meets all of these requirements is the composite spline

$$\lambda_1(M) \equiv \begin{cases} 1 - M + \dfrac{\varepsilon_M}{2}(2M)^{1/\varepsilon_M}, & 0 \leqslant M < \frac{1}{2} \\ \dfrac{(M - \frac{1}{2})^2}{2\varepsilon_M} + \dfrac{1 + \varepsilon_M}{2}, & \frac{1}{2} \leqslant M < \frac{1}{2} + \varepsilon_M \\ M, & \frac{1}{2} + \varepsilon_M \leqslant M \end{cases} \tag{64}$$

### 6.4. Upstream-bias functions $a$, $\alpha$, $\delta$ and $\alpha^N$

These functions are used in actual computations based on the characteristics flux divergence (53). In the eigenvalues $\lambda_{1,2}$ in (59), the components

$$n_i \alpha a_i a_j n_j = \alpha(a_j n_j)^2, \quad n_i \alpha^N a_i^N a_j^N n_j = \alpha^N(a_j^N n_j)^2 \tag{65}$$

are already non-negative for non-negative $\alpha$ and $\alpha^N$. The eigenvalues $\lambda_{1,2}$, therefore, will remain non-negative for all positive $\alpha$ and $\alpha^N$, including $\alpha \to 0$ and $\alpha^N \to 0$, when the additional component $n_i a_i v_j n_j M$ remains non-negative for all $M$. This requirement is met along with the first condition in (62) when $\mathbf{a} = \mathbf{v}$, for

$$n_i a_i v_j n_j M = M(v_j n_j)^2 \geqslant 0 \tag{66}$$

This finding is not surprising, for the streamline direction is a principal characteristic direction.

From $\lambda_1$ and $\lambda_4$ in (60), the corresponding expressions for both $\alpha = \alpha(M)$ and $\delta = \delta(M)$ are then directly and exactly determined as

$$\alpha(M) = \lambda_1(M) - M, \quad \delta(M) = \frac{(\lambda_1(M) - \lambda_4(M))(\lambda_1(M) - \lambda_4(M) + p_E M)}{1 + p_E M(\lambda_1(M) - \lambda_4(M))} \tag{67}$$

where according to the third and fourth conditions in (62) the streamline eigenvalues $\lambda_4$ and $\lambda_1$ are, respectively, given by (63), (64).

For the determination of $\alpha^N = \alpha^N(M)$ from $\lambda_{3,4}(M,\mathbf{n}) \geqslant 0$ in (62), note that $\mathbf{a} = \mathbf{v}$ remains perpendicular to $\mathbf{a}^N$, while $n_i a_i$ and $n_i a_i^N$ denote the vector 'dot' products between the unit vector $\mathbf{n}$ and the unit vectors $\mathbf{a}$ and $\mathbf{a}^N$, respectively. Accordingly,

$$n_i a_i = \cos \bar{\theta}, \quad n_i a_i^N a_j^N n_j = \sin^2 \bar{\theta}, \quad \bar{\theta} \equiv \theta - \theta_{\mathbf{v}} \tag{68}$$

where $\theta$ and $\theta_{\mathbf{v}}$ denote the inclination angles between the $x_1$-axis and $\mathbf{n}$ and $\mathbf{v}$, respectively.

For eigenvalue $\lambda_4 = \lambda_4(M,\mathbf{n})$ in (59), therefore, the condition $\lambda_4(M,\mathbf{n}) \geqslant 0$ yields

$$\alpha^N \geqslant g(\bar{\theta},M) \equiv \frac{\cos \bar{\theta} \sqrt{(((1-\delta)/2) p_E \cos \bar{\theta} M)^2 + \delta} - \cos^2 \bar{\theta}(\alpha + (1 + ((1-\delta)/2) p_E)M)}{1 - \cos^2 \bar{\theta}} \tag{69}$$

For supersonic flows with $M \geqslant 1 + \varepsilon_M$, $\alpha = 0$ and $\delta = 1$, hence (69) becomes

$$\alpha^N \geqslant g(\bar{\theta},M) = \frac{\cos \bar{\theta} - M \cos^2 \bar{\theta}}{1 - \cos^2 \bar{\theta}} \tag{70}$$

and in particular $\alpha^N \geqslant g_{\max}(M)$, where $g_{\max}(M)$ denotes the maximum of $g = g(\bar{\theta},M)$ with respect to $\bar{\theta}$, for each $M$. From (70), the determination of $g_{\max}(M)$ yields

$$\frac{\partial g}{\partial \bar{\theta}} = 0 \quad \Rightarrow \quad \cos^2 \bar{\theta} - 2M \cos \bar{\theta} + 1 = 0 \tag{71}$$

which leads to

$$\cos \bar{\theta}|_{g=g_{\max}} = M - \sqrt{M^2 - 1}, \quad g_{\max}(M) = \tfrac{1}{2}(M - \sqrt{M^2 - 1}) \tag{72}$$

Significantly, the same solution for $g_{\max}(M)$ results from the condition $\lambda_3(M,\mathbf{n}) \geqslant 0$. Consequently,

$$\alpha^N \geqslant \tfrac{1}{2}(M - \sqrt{M^2 - 1}), \quad M \geqslant M_M \equiv 1 + \varepsilon_M \tag{73}$$

and considering that $\lambda_4(1,\mathbf{v}) = \varepsilon_M/2$, an analogous equality is adopted for $\alpha^N(M_M)$, leading to $\alpha^N(M_M) = g_{\max}(M_M) + \varepsilon_M/2$.

For subsonic flows, a numerical analysis of $g = g(\bar{\theta},M)$ from (70) reveals that $g(\bar{\theta},M) < 0.3$ for all $\bar{\theta}$ and $M < M_M$. Additionally, for an isotropic acoustic upstream for vanishing $M$, $\alpha^N(0) = 1$ and $\partial \alpha^N/\partial M|_{M=0} = 0$, whereas for $M \geqslant M_M$ both $\alpha^N$ and its derivative with respect to $M$ follow from (73). A smooth variation for $\alpha^N = \alpha^N(M)$ that satisfies $\lambda_{3,4}(M,\mathbf{n}) \geqslant 0$ in (62) along with all of these constraints is the composite spline

$$\alpha^N(M) \equiv \begin{cases} (\alpha_M^{N'} M_M - 2\alpha_M^N + 2)\left(\dfrac{M}{M_M}\right)^3 - (\alpha_M^{N'} M_M - 3\alpha_M^N + 3)\left(\dfrac{M}{M_M}\right)^2 + 1, & 0 \leqslant M < M_M \\[2mm] \dfrac{1}{2}\left(1 + \dfrac{\varepsilon_M}{M_M - \sqrt{M_M^2 - 1}}\right)(M - \sqrt{M^2 - 1}), & M_M \leqslant M \end{cases} \tag{74}$$

where superscript prime '$'$' denotes differentiation with respect to $M$ and subscripts '$M$' in both $\alpha_M^{N'}$ and $\alpha_M^N$ indicate their respective magnitudes at $M = M_M$ from the second expression in (74).

## 6.5. *Variations of streamline eigenvalues and upstream-bias functions*

As Figure 4 shows, the streamline upstream-bias eigenvalues $\lambda_{1,2}$ as well as $\lambda_4$, respectively, from (64), (63), and $\lambda_3$, from (60), remain positive. Furthermore, these eigenvalues and their slopes remain continuous for all Mach numbers. For $0 \leqslant M \leqslant 1 + \varepsilon_M$, the eigenvalues $\lambda_{1,2}$, $\lambda_3$, $\lambda_4$ smoothly approach 1 for vanishing $M$, indicating a physically consistent upstream-bias approximation of the acoustic equations with matrix (39) embedded within the Euler equations. For $M > 1 + \varepsilon_M$, these eigenvalues, respectively, coincide with the Euler flux Jacobian streamline eigenvalues $M$, $M + 1$, $M - 1$, which corresponds to a streamline upstream-bias approximation of the entire flux vector, for supersonic flows. A smooth transition takes place in the critical sonic region within a transonic layer, where $\lambda_4$ does not vanish, but remains not less than $\varepsilon_M/2$.

The variations of $\alpha = \alpha(M)$, $\alpha^N = \alpha^N(M)$ and $\delta = \delta(M)$ in Figure 5 indicate that these three functions as well as their slopes remain continuous for all Mach numbers.

This figure indicates that $0 \leqslant \alpha, \alpha^N, \delta \leqslant 1$ and $\alpha \equiv 0$ for $M > \frac{1}{2} + \varepsilon_M$, $\delta \equiv 0$ for $M \leqslant 0.4$, and $\delta \equiv 1$ for $M > 1 + \varepsilon_M$. The variation of $\delta = \delta(M)$ shows that the pressure-gradient contribution to this upstream-bias formulation increases monotonically, while remaining less than 25% of its maximum, for $0 \leqslant M \leqslant 0.7$. As $\delta = \delta(M)$ rises, the streamline upstream bias $\alpha$ contribution from the corresponding acoustics matrix decreases rapidly, reducing by 75% at $M = 0.39$.

The decrease of $\alpha^N$, hence of the crossflow upstream bias is less rapid because this is the only contribution to a crossflow upstream. The function $\alpha^N$, nevertheless, decreases by 50%, at the sonic state, and by 80% for $M = 1.8$. For this function, forcing non-negativity of $\lambda_{3,4}$ as opposed to equality to a prescribed positive constant, in particular, ensures minimal crossflow
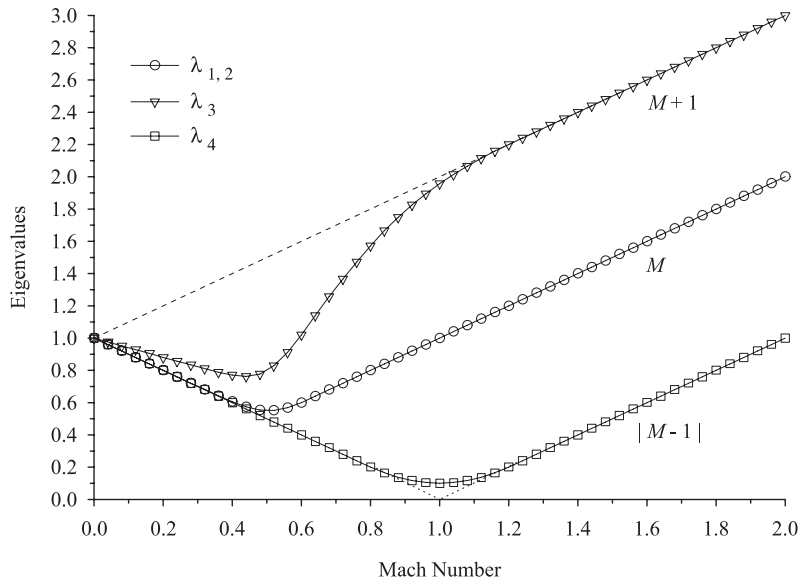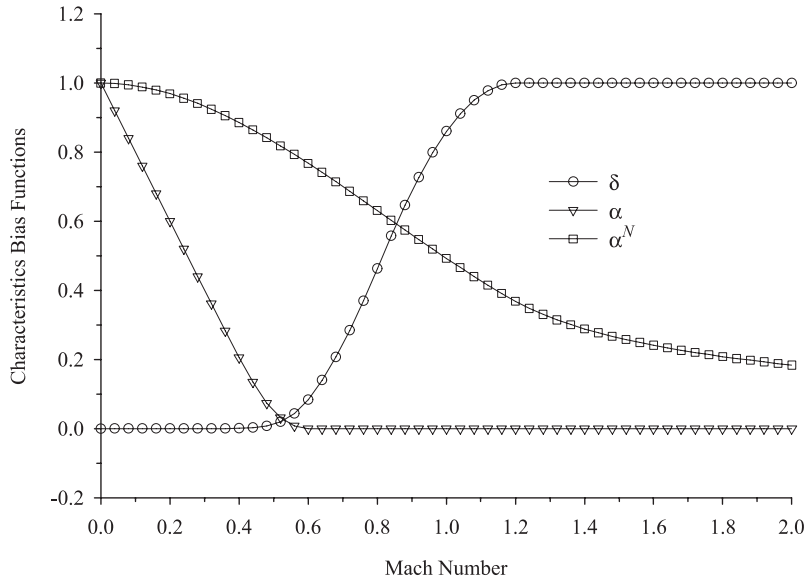


Figure 4. Upstream-bias eigenvalues.

Figure 5. Upstream-bias functions.

diffusion. Expression (74) leads to the conclusions

$$\lim_{M \to \infty} \alpha^N(M) = 0, \quad \lim_{M \to \infty} \frac{\partial \alpha^N}{\partial M} = 0 \tag{75}$$

which indicate that the magnitude of crossflow upstream decreases with increasing $M$. This result agrees with the physics of high-$M$ flows, where the bi-modal propagation region narrows about the crossflow direction. Convection thereby becomes the prevailing wave propagation mechanism, which therefore reduces the need for acoustic crossflow upstream bias.

### 6.6. Polar variation of upstream bias

Figures 6–9 present the directional variation of the upstream bias eigenvalues (59) for representative subsonic and supersonic Mach numbers. These variations are obtained for a variable unit vector $\mathbf{n} \equiv (\cos \theta, \sin \theta)$ and fixed unit vector $\mathbf{a} = \mathbf{v}$, in this representative case inclined by $+30°$ with respect to the $x_1$-axis.

These figures collectively indicate that the characteristics flux divergence (53) induces a physically consistent upstream bias because for any Mach number and wave propagation direction $\mathbf{n}$ the associated upstream-bias eigenvalues (59) remain positive and their directional variation mirrors the directional variation of the characteristic Euler eigenvalues (15). The upstream-bias eigenvalues, moreover, are symmetrical about the crossflow direction and characteristic streamline, precisely like the characteristic Euler eigenvalues. For $M = 0.05$, the directional variation of the upstream-bias eigenvalues in Figure 6 correlates with that in Figure 2 and thereby corresponds to an isotropic upstream bias, in complete agreement with the isotropic acoustic wave propagation speed in the Euler equations.
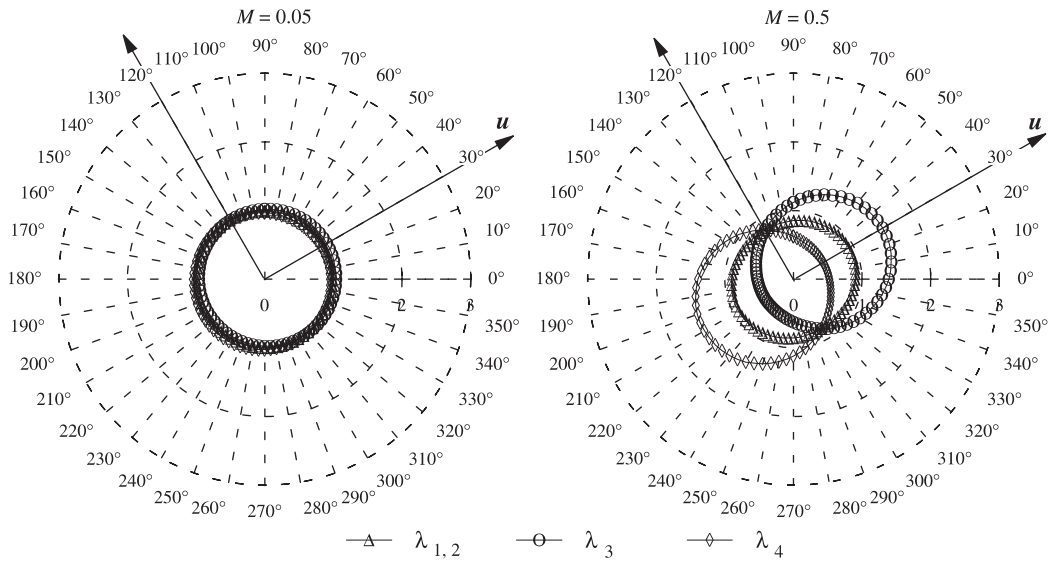
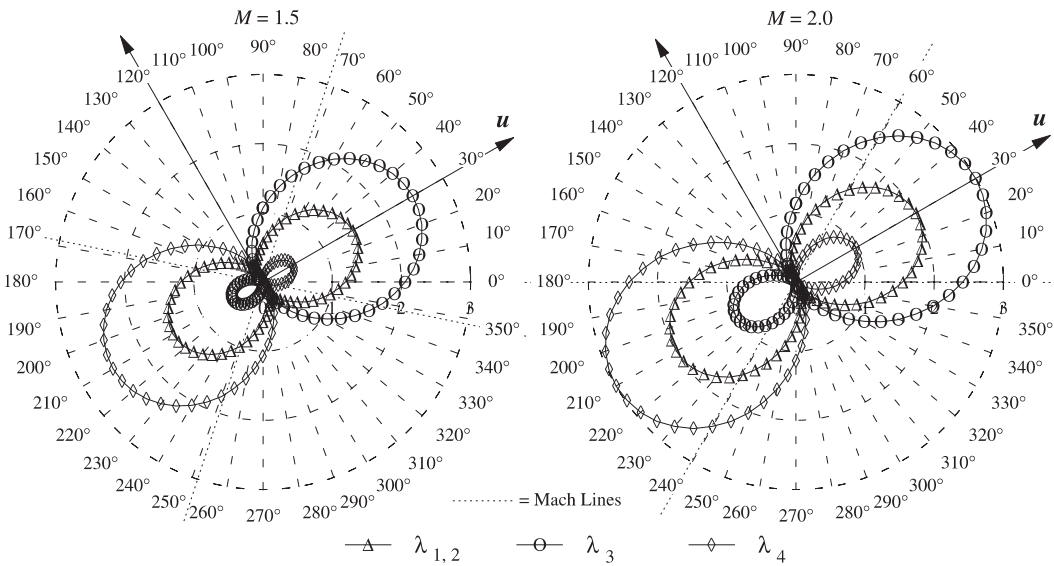Figure 6. Polar variation of subsonic upstream bias.



Figure 7. Polar variation of supersonic upstream bias.

For increasing Mach numbers, the upstream bias becomes anisotropic, again in agreement with the anisotropic distribution of the Euler eigenvalues (14). For $M = 0.5$ this anisotropy is already evident and then becomes more marked for supersonic Mach numbers as indicated in Figure 7, which correlates with Figure 3. In particular, the crossflow upstream bias decreases for increasing Mach number.
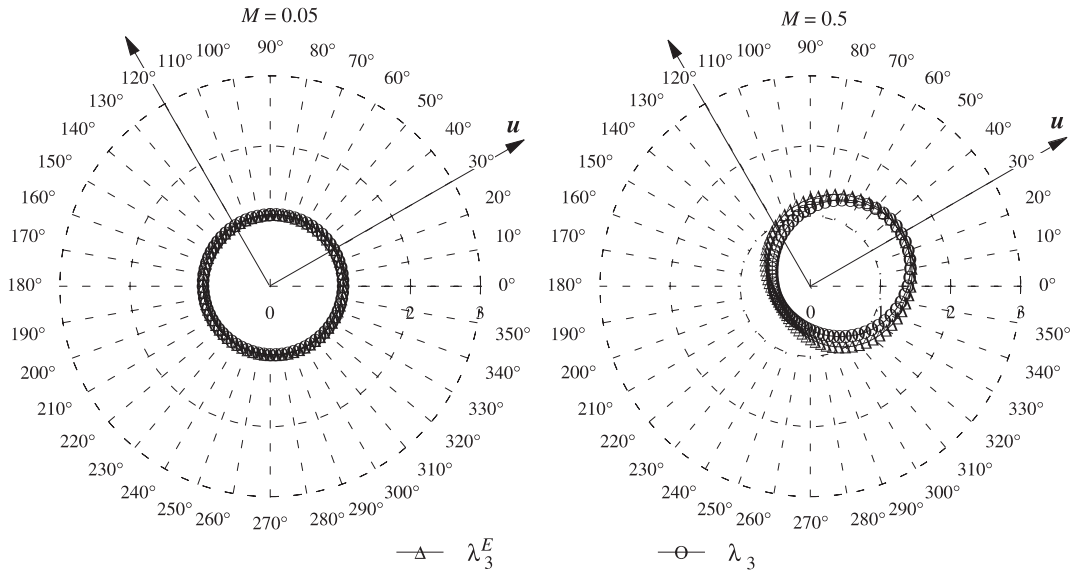
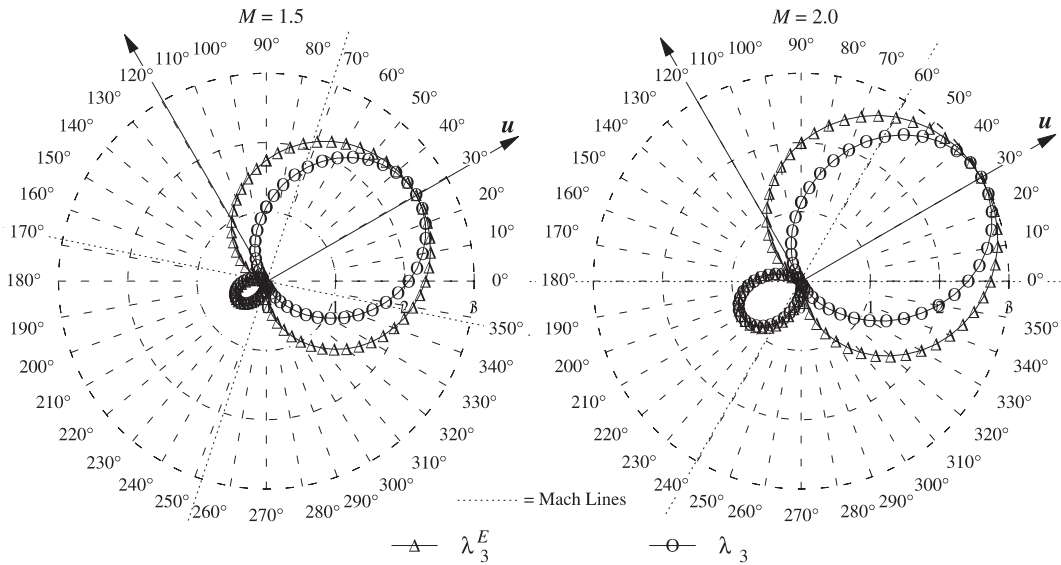Figure 8. Polar correlation of subsonic characteristic $\lambda_3^E$ and upstream $\lambda_3$.



Figure 9. Polar correlation of supersonic characteristic $\lambda_3^E$ and upstream $\lambda_3$.

Figures 8 and 9 compare the directional variations of the representative upstream-bias eigenvalue $\lambda_3$ and the corresponding Euler eigenvalue $\lambda_3^E$. This comparison is sufficient to depict the correlation between all the Euler and upstream-bias eigenvalues, for $\lambda_{1,2}$ and $\lambda_{1,2}^E$ are topologi-

cally similar to each other, compare Figures 3 and 7, while $\lambda_4$ and $\lambda_4^E$ are, respectively, mirror skew-symmetric to $\lambda_3$ and $\lambda_3^E$ with respect to the crossflow direction. As Figures 8 and 9 indicate, $\lambda_3$ is symmetrical about the characteristic streamline, precisely like the corresponding characteristic Euler eigenvalue $\lambda_3^E$ and the corresponding polar curve is topologically similar to the Euler eigenvalue curve. For $M = 0.05$, $\lambda_3$ and $\lambda_3^E$ virtually coincide with each other and remain direction invariant, which corresponds to an isotropic upstream bias in correlation with the acoustic speed. For $M = 0.5$, Figure 8 indicates that $\lambda_3^E$ is greater than $\lambda_3$ in the streamline direction.

For supersonic Mach numbers, $\lambda_3$ in the streamline direction coincides with $M + 1$. As shown in Figure 9, therefore, the magnitude of the upstream bias for supersonic flows is virtually identical to the magnitude of the characteristic eigenvalues, within the domain of dependence and range of influence of any flow field point.

Outside this region, the upstream-bias eigenvalues are modestly less than the characteristic eigenvalues. In these variations, the upstream-bias eigenvalues are vanishingly small in the cross-flow direction, which, in particular, corresponds to minimal crossflow diffusion.

## 7. CONCLUDING REMARKS

This paper has presented an acoustics–convection upstream resolution formulation computationally to solve the Euler and Navier–Stokes equations with general equilibrium equations of state. Relying upon the physics and mathematics of multi-dimensional characteristic acoustics and convection, the formulation induces the upstream bias directly at the differential equation level, before any discrete approximation, by way of a characteristics-bias system and associated decomposition of the Euler flux Jacobian into convection and streamline as well as crossflow acoustic components. As the second paper of this series details, a traditional Galerkin finite element discretization of the characteristics-bias system directly provides a genuinely multi-dimensional upstream-bias approximation of the Euler and Navier–Stokes equations.

The magnitude of the streamwise and crossflow upwind dissipations in this formulation remain different from and independent of each other; the streamwise dissipation increases with the Mach number whereas the crossflow dissipation decreases with increasing Mach number. The acoustics–convection upstream resolution algorithm provides an intrinsically multi-dimensional upstream-bias approximation for the Euler equations and along all the infinite directions of wave propagation, the formulation induces anisotropic and variable-strength consistent upwinding that correlates with the spatial distribution of characteristic velocities.

### REFERENCES

1. Iannelli J. Finite element and implicit Runge–Kutta implementation of an acoustics convection upstream resolution algorithm for the time-dependent two-dimensional Euler equations. *International Journal for Numerical Methods in Fluids* 2005, this issue.
2. Baker AJ, Kim JW. A Taylor weak statement algorithm for hyperbolic conservation laws. *International Journal for Numerical Methods in Fluids* 1987; **7**:489–520.
3. Luo H, Baum JD, Löhner R, Cabello J. Adaptive edge-based finite element schemes for the Euler and Navier–Stokes equations on unstructured grids. *AIAA Paper 93-0336*, 1993.
4. Hughes TJR, Brooks A. A theoretical framework for Petrov–Galerkin methods with discontinuous weighting functions: application to the streamline-upwind procedure. *Finite Elements in Fluids*, vol. IV. Wiley: New York, 1982; 47–65.

5. Hughes TJR. Recent progress in the development and understanding of SUPG methods with special reference to the compressible Euler and Navier–Stokes equations. *International Journal for Numerical Methods in Fluids* 1987; **7**:11–21.
6. Johnson C. *Numerical Solution of Partial Differential Equations by the Finite Element Method*. Cambridge University Press: Cambridge, 1987.
7. Johnson C, Szepessy A. On the convergence of a finite element method for a nonlinear hyperbolic conservation law. *Mathematics of Computation* 1987; **180**(49):427–444.
8. Johnson C, Szepessy A, Hansbo P. On the convergence of shock-capturing streamline diffusion finite element methods for hyperbolic conservation laws. *Mathematics of Computation* 1990; **189**(54):107–129.
9. Carette J-C, Deconinck H, Paillere H, Roe PL. Multidimensional upwinding: its relation to finite elements. *International Journal for Numerical Methods in Fluids* 1995; **20**:935–955.
10. Davis SF. A rotationally-biased upwind difference scheme for the Euler equations. *Journal of Computational Physics* 1984; **56**:65–92.
11. Levy DW, Powell KG, van Leer B. Use of a rotated Riemann solver for the two-dimensional Euler equations. *Journal of Computational Physics* 1993; **106**:201–214.
12. Dadone A, Grossman B. A rotated upwind scheme for the Euler equations. *AIAA Paper 91-0635*, 1991.
13. Coirier W, van Leer B. Numerical flux formulas for the Euler and Navier–Stokes equations: II. Progress in flux-vector splitting. *AIAA Paper 91-1566*, 1991.
14. Rumsey CL, van Leer B, Roe PL. A multidimensional flux function with applications to the Euler and Navier–Stokes equations. *Journal of Computational Physics* 1993; **105**:306–323.
15. Parpia IH. A planar oblique wave model for the Euler equations. *AIAA Paper 91-1545-CP*, 1991.
16. Paillere H, Deconinck H, Struijs R, Roe PL, Mesaros LM, Muller JD. Computations of inviscid compressible flows using fluctuation-splitting on triangular meshes. *AIAA Paper 93-3301*, 1993.
17. Roe PL. Beyond the Riemann problem: part I. *Algorithmic Trends in CFD*. Springer: Berlin, 1993.
18. Iannelli J. A CFD Euler solver from a physical acoustics–convection flux Jacobian decomposition. *International Journal for Numerical Methods in Fluids* 1999; **31**:821–860.
19. White FM. *Viscous Fluid Flow* (3rd edn). McGraw-Hill: New York, 2005.
20. Hirsch C. *Numerical Computation of Internal and External Flows*, vols. 1, 2. Wiley: New York, 1991.
21. Garabedian PR. *Partial Differential Equations*. Chelsea Publishing Company: New York, 1986.
22. Zauderer E. *Partial Differential Equations of Applied Mathematics*. Wiley: New York, 1989.
23. Oden JT, Reddy JN. *An Introduction to the Mathematical Theory of Finite Elements*. Wiley: New York, 1976.
24. Hutson V, Pym JS. *Applications of Functional Analysis and Operator Theory*. Academic Press: New York, 1980.
25. Vincenti WG, Kruger Jr CH. *Introduction to Physical Gas Dynamics*. Wiley: New York, 1965.
26. Horn RA, Johnson CR. *Matrix Analysis*. Cambridge University Press: Cambridge, 1991.